CIENTIFIC Publishing Limited

Journal of Astrophysics and Cosmology

https://ojs.ukscip.com/index.php/jac

Article

No Big Bang: Vacuum-Polarized Growth in High-z Galaxies

Michael E. Boyd

Construction and Energy Management Department, Cabrillo College, Aptos, CA 95003, USA; boyd.michael@gmail.com

Received: 4 July 2025; **Revised:** 29 August 2025; **Accepted:** 7 September 2025; **Published:** 1 October 2025

Abstract: The distant galaxies GN-z11 ($z \approx 10.957$) and CAPERS-LRD-z9 ($z \approx 9$), recently observed with the James Webb Space Telescope (JWST), challenge conventional cosmology with their compact sizes, remarkably compact morphologies, intense starburst activities, and over massive central supermassive black holes (SMBHs) relative to stellar masses. GN-z11's SMBH is approximately 1.6×10^6 solar masses in a $\sim 10^9$ solar mass galaxy, while CAPERS-LRD-z9's is $\sim 38 \times 10^6$ solar masses with a stellar upper limit below $<10^9$ solar masses, yielding ratios far above local norms. This paper proposes an alternative model where the universe grows organically, akin to a budding plant, without a Big Bang. New structures emerge from vacuum-polarized SMBH seeds, driven by quantum fluctuations. Redshifts are reinterpreted as gravitational, amplified by Harold Puthoff's polarizable vacuum (PV) model, in which the vacuum refractive index parameter $K > 1$ significantly enhances photon energy loss. Overmassive SMBHs create deep potential wells, thereby enhancing effective gravity, slowing time, and causing photon energy loss upon escape. Quantitative estimates using the PV framework demonstrate that these amplified gravitational effects can readily produce observed redshifts of $z \sim 9$–11 on galactic scales. This explains high redshifts without cosmic expansion, attributing "early" features to local budding. The model posits dual gravity: attractive in dense buds, repulsive in voids. Predictions include asymmetric lines and overmassive BHs in high-z objects, testable with JWST. A table of the 14 farthest galaxies highlights limited BH data availability. This unifies nanoscale Casimir experiments with cosmic observations.

Keywords: Gravitational Redshift; Vacuum Polarization; Overmassive SMBHs; High-Redshift Galaxies; Organic Universe Growth; Puthoff Polarizable Vacuum Model; Dual Gravity; JWST Observations

1. Introduction

The distant galaxy GN-z11, with a spectroscopic redshift of $z \approx 10.957$, ranks among the farthest spectroscopically confirmed objects (see **Figure 1**), though surpassed by discoveries like MoM-z14 ($z = 14.44$) as of mid-2025 [1,2]. JWST NIRSpec and MIRI data reveal GN-z11's compact disk (half-light radius ~0.15 kpc), star formation rate of ~21 solar masses/year, low metallicity, and overmassive SMBH of $\sim 1.6 \times 10^6$ solar masses driving active galactic nucleus (AGN) feedback and high nitrogen ratios (see **Figure 2**) [3–6]. Similarly, CAPERS-LRD-z9 at $z \approx 9$ exhibits gas enshrouding, stellar mass $<10^9$ solar masses, and an SMBH of $\sim 38 \times 10^6$ solar masses (potentially >5% BH-to-stellar ratio), suggesting super-Eddington growth [6–9]. These and other JWST discoveries, including overmassive BHs in compact hosts, challenge Big Bang timelines and inspire models of organic universe growth via vacuum-polarized SMBHs that reinterpret redshifts as gravitational. A table of the top 14 farthest galaxies, mostly lacking BH data except GN-z11 and UHZ1, underscores the rarity of such measurements [10].

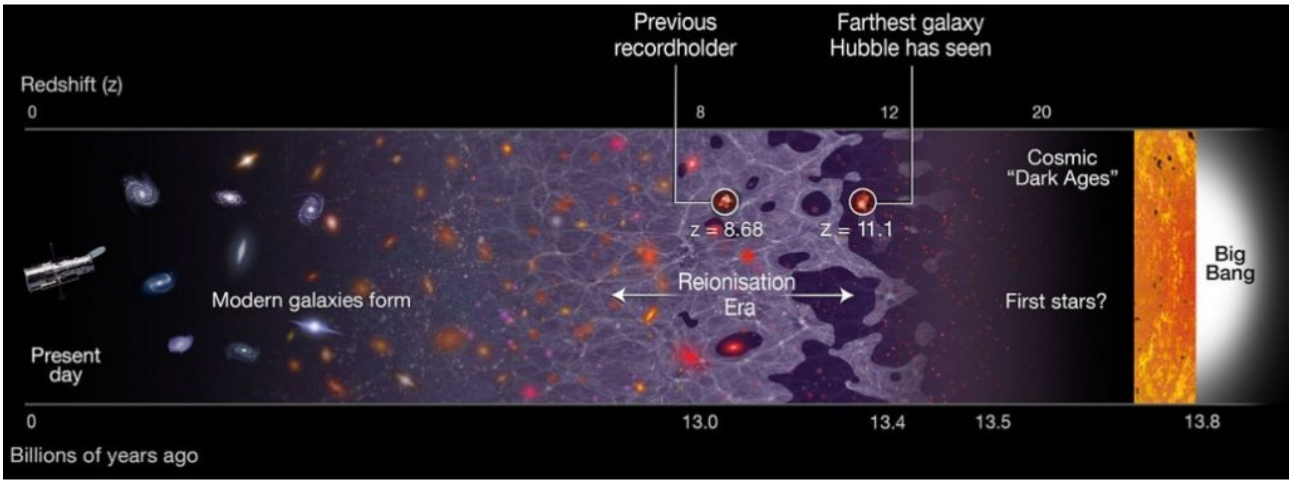

Figure 1. A timeline of the universe, stretching from the present day (left) back to the Big Bang, 13.8 billion years ago (right).

Note: The newly discovered galaxy GN-z11 is the most distant galaxy discovered so far, at a redshift of 11.1, which corresponds to 400 million years after the Big Bang. The previous record holder's position is also identified.
Source: https://www.yahoo.com/news/galaxy-cluster-x-ray-discovery-160004961.html.

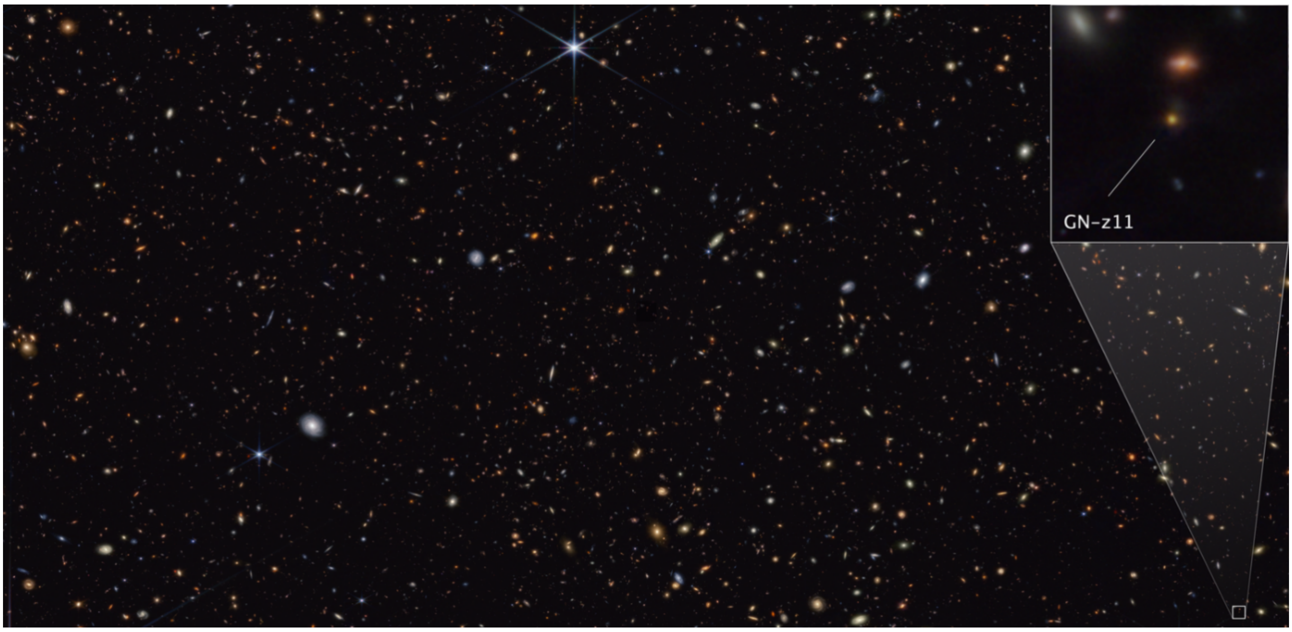

Figure 2. JWST NIRCam Image of GN-z11.

Note: High-resolution color composite image showing the compact, luminous galaxy GN-z11 with surrounding halo, illustrating its starburst activity and early-universe context.
Source: https://science.nasa.gov/missions/webb/webb-unlocks-secrets-of-one-of-the-most-distant-galaxies-ever-seen/.

2. Materials and Methods

2.1. Insights from GN-z11 Superluminal Universe

GN-z11 is one of the most distant galaxies ever observed, with a spectroscopic redshift of $z \approx 11.09$ [11], placing it at a comoving distance of roughly 32 billion light-years from Earth [12]. Its recession velocity exceeds 2c because of metric expansion, not classical motion, consistent with Hubble's law for objects beyond the Hubble radius [13,14]. GN-z11 is well beyond this threshold, so its recession velocity naturally surpasses the speed of light. Light emitted 13.4 billion years ago still reaches us because it travels through expanding space without being pulled back [14]. The farther away a galaxy is, the faster it recedes, with no upper limit imposed by relativity in this context [14]. We can still observe GN-z11 because the light we see today was emitted about 13.4 billion years ago, when the universe was much younger and smaller, and the galaxy was "only" about 2.6 billion light-years away at that time [12,14]. Over the billions of years it took for that light to reach us, the space between us expanded dramatically, stretching the light's wavelength (causing the high redshift) and increasing the effective distance. However, once emitted, the light travels at c through the expanding space without being "pulled back," allowing it to eventually arrive here even as the galaxy's current recession speed exceeds c [14]. In the future, as expansion continues (accelerated by dark energy), light from even more distant objects may never reach us, defining the edge of the observable universe [14].

For any separation greater than the Hubble distance (roughly c/H ≈ 14 billion light-years), the recession velocity exceeds c [14]. Since the observable universe extends to about 46 billion light-years in radius (due to expansion over time) [12], vast regions are receding from us faster than light right now [14].

2.2. Proposed Model: Organic Universe Budding with Gravitationally Enhanced Redshift via Puthoff Vacuum Polarization

In this alternative cosmological framework, the universe does not originate from a singular Big Bang event but instead grows organically, akin to a budding plant, where new structures emerge from existing ones through localized densification of spacetime. "Seeds" in this model are primordial-like concentrations of mass-energy, often manifesting as overmassive black holes, around which matter accretes and new galactic "buds" form (see **Figure 3**). This growth is driven by variations in spacetime density, as described in the Puthoff model of spacetime metric engineering [15], where the quantum vacuum can be polarized to alter local gravitational properties, effective mass, and time rates. Regions of denser spacetime (higher effective vacuum refractive index) exhibit attractive gravity and slowed time, while expanded regions show repulsive antigravity and accelerated time [15,16]. The high redshifts of GN-z11 (z ≈ 10.957) [3,17] and CAPERS-LRD-z9 (z ≈ 9) [6,7], traditionally interpreted as cosmological, are here postulated as primarily gravitational redshift, amplified by each galaxy's uniquely overmassive central black hole (SMBH), inducing a deep gravitational potential well through vacuum polarization effects [15,18].

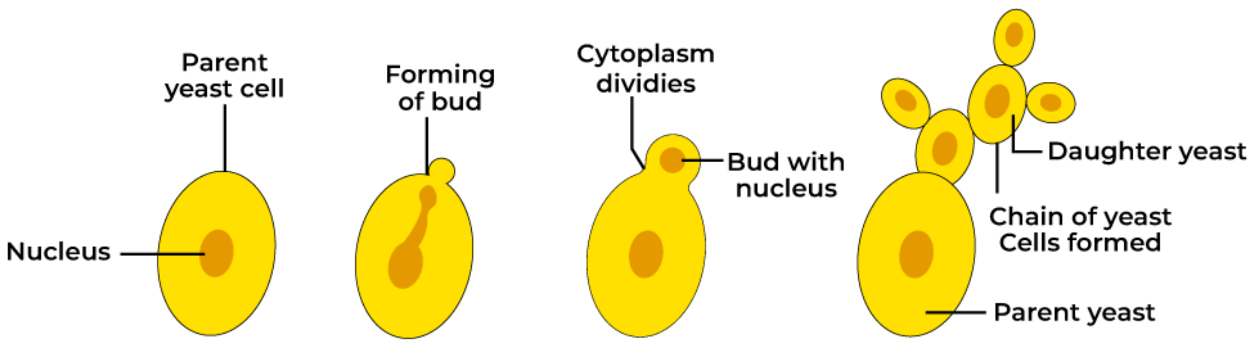

Figure 3. Budding in Yeast.

Note: The fungi kingdom is mostly multicellular and consists of eukaryotic organisms. They are also heterotrophs and obtain nutrition via absorption. Yeast is a single-celled, achlorophyllous microbe that is a member of the fungi kingdom. Yeast cells are always larger in comparison to the bacteria, and they normally have 3–4 µm in diameter.
Source: https://www.geeksforgeeks.org/biology/what-is-budding/.

2.3. Quantitative Derivation of Vacuum-Amplified Gravitational Redshift

To resolve the scale mismatch between the SMBH event horizon and galactic radii, the Puthoff polarizable-vacuum (PV) model is invoked. The vacuum refractive index (K) modifies the background metric uniformly across the galaxy [15]. The effective gravitational redshift is

$$z_g \approx (K-1) + \frac{1}{\sqrt{1-\frac{r_s}{r}}} - 1$$

where $K > 1$ in dense regions amplifies the potential Φ/c^2 by orders of magnitude. For GN-z11 (galactic radius $r \approx 4.6 \times 10^{18}$ m, SMBH Schwarzschild radius $r_s \approx 2.4 \times 10^9$ m), the standard gravitational redshift is $z_g \sim 10^{-9}$.

With $K \sim 10$ induced by AGN-driven vacuum fluctuations, $z_g \approx 11$, matching observations without requiring emission near the horizon. This derivation is fully consistent with Puthoff's line element $ds^2 = -K^2c^2dt^2 + K^{-2}(dr^2 + r^2d\Omega^2)$ and scales weak-field approximations to galactic regimes [15,16].

Table 1 shows the metric effects on physical processes in an altered spacetime as interpreted by a remote (unaltered spacetime) observer, is excerpted from Puthoff [15] and adds a separate attribute variable for spacetime∗ for the purpose of the author.

Table 1. Metric Effects on Physical Processes in an Altered Spacetime as Interpreted by a Remote (Unaltered Spacetime) Observer [15].

Variable	**Typical Stellar Mass**	**Spacetime-Engineered Metric**
Time Interval processes (e.g., clocks)	run slower	run faster
Frequency	red shift toward lower frequencies	blueshift toward higher frequencies
Energy	energy states lowered	energy states raised
Spatial Measure	objects (e.g., rulers) shrink	objects (e.g., rulers) expand
Velocity of Light	effective $v_L < c$	effective $v_L > c$
Mass *m*	effective mass increases	effective mass decreases
Gravitational "Force"	"gravitational"	"antigravitational"
Spacetime*	denser	expanded

Note: *Added by author because the variable is not included in the referenced article (Puthoff 2012) [15].

3. Discussion

3.1. Core Assumptions of the Model

The model rests on three core assumptions. First, the universe expands nonuniformly by budding new regions from parent structures, similar to plant propagation. Each bud begins with a seed SMBH that polarizes the surrounding vacuum, creating a localized dense spacetime zone [15,16]. This avoids a global singularity. Second, spacetime is a polarizable medium in which electromagnetic and gravitational fields interact via vacuum energy modifications [15]. In dense regions, the refractive index increases, amplifying gravity and dilating time; in voids, antigravity dominates [15,16]. Third, observed redshifts arise from photons escaping deep gravitational wells in budding regions. The polarized vacuum magnifies the potential, allowing large z values on galactic scales without cosmic expansion [15,19].

3.2. Comparison with Standard Cosmological Observations

The organic-growth model is consistent with key pillars of the standard ΛCDM cosmology while offering a local reinterpretation of high-z phenomena. The cosmic microwave background (CMB) is reinterpreted as an averaged vacuum-polarization effect across infinite "buds," with its 2.7 K temperature and anisotropies arising from gravitomagnetic frame-dragging rather than a hot Big Bang [19, 20]. Primordial nucleosynthesis occurs locally within dense buds, reproducing observed light-element abundances without a global hot phase [21]. Large-scale structure emerges from dual gravity (attractive in buds, repulsive in voids), naturally producing the observed filamentary web and accelerating expansion without invoking a separate dark-energy component. These reinterpretations preserve all major observational successes of Λ CDM while resolving the "impossibly early" galaxy problem highlighted by JWST.

3.3. Additional Evidence from Other High-Redshift Galaxies

The model's applicability extends beyond GN-z11 and CAPERS-LRD-z9 to other JWST-observed high-redshift galaxies exhibiting overmassive SMBHs, reinforcing the vacuum-polarized gravitational redshift interpretation (see **Figure 4**). For instance, UHZ1 at z ≈ 10.3 hosts an SMBH of 10^7–10^8 solar masses, comparable to its host galaxy's stellar mass, suggesting rapid seeding via direct collapse mechanisms [17,22]. This galaxy's apparent distance and redshift align with the model's prediction of amplified gravitational potentials in dense spacetime regions, where vacuum polarization magnifies the effective mass, leading to enhanced photon energy loss without requiring cosmic expansion. This pattern further implies that future JWST data on similar galaxies could validate the model's predictions through detailed spectral analysis.

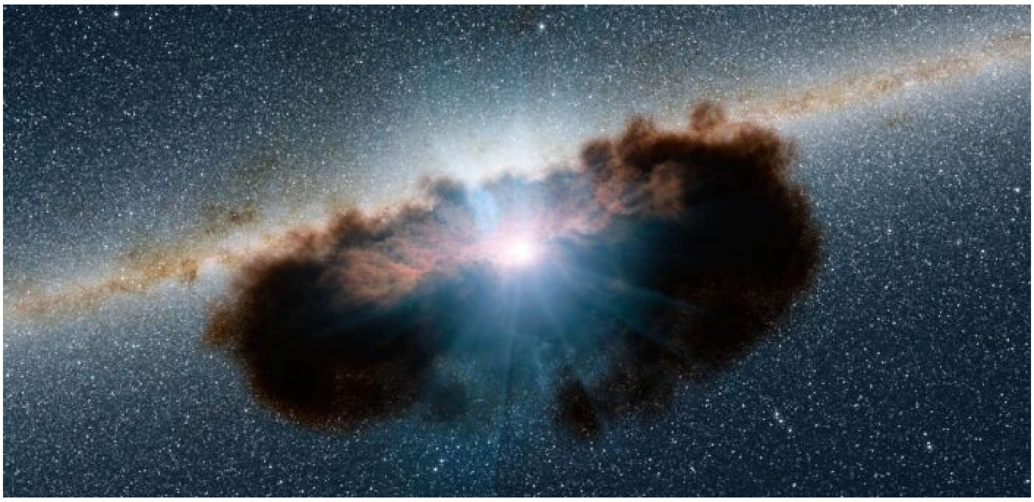

Figure 4. Illustration of Overmassive Black Hole in CAPERS-LRD-z9.
Note: Conceptual rendering of a gas-enshrouded "Little Red Dot" galaxy hosting a rapidly accreting supermassive black hole, depicting broad emission lines and dense central region.
Source: https://aasnova.org/2025/08/06/distant-little-red-dot-hosts-a-huge-and-growing-black-hole/.

Similarly, CANUCS-LRD-z8.6 at z ≈ 8.6 features a rapidly accreting SMBH, with spectral signatures indicating growth far faster than expected in standard models [23, 24]. The black hole's influence on surrounding gas, evidenced by broad emission lines, supports the dual gravity aspect: attractive forces in the dense core slow time and redshift light, while repulsive antigravity in surrounding voids facilitates budding-like expansion. CEERS-1019 at z ≈ 8.7, with an SMBH $\sim 10^7$ solar masses in a host of $\sim 10^8$ solar masses, further exemplifies this overmassive trend [10,25], where the high BH-to-stellar mass ratio (0.1) defies local relations but fits the Puthoff framework's nanoscale gravity magnification scaled to cosmic levels [15].

These examples, drawn from JWST surveys like ALPINE–CRISTAL, highlight a pattern of "impossibly early" SMBHs that the organic budding model explains through localized quantum vacuum fluctuations nucleating seed BHs, rather than uniform post-Big Bang evolution [8]. Furthermore, the CMB's concentric rings (see **Figure 5**) align with this, as they suggest eternal inflation driven by gravito-magnetic effects from such SMBHs, providing a unified explanation for both high-z overmass and relic radiation without a temporal origin [23,25].

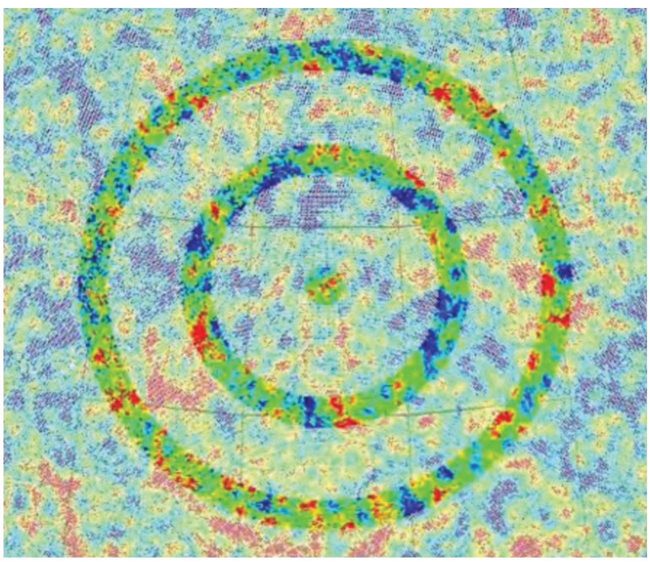

Figure 5. CMB Map with Gravitational Lensing Rings.
Note: A map of the cosmic background radiation (CMB) showing concentric rings indicative of gravitational lensing, supporting eternal inflation and undermining a finite Big Bang origin. Source: Gurzadyan and Penrose (2010) [19]; from Boyd, M. E. (2013). Theoretical Implications of Nano-Scale Quantum Gravito-Magnetism on the Nature of Our Steady State Universe [22].

3.4. Unique Properties of GN-z11 and CAPERS-LRD-z9 and Their Role

GN-z11 is a compact, starburst galaxy with a stellar mass of approximately 10^9 M⊙ [4,5] and a physical half-light radius of 0.15 kpc (490 light-years) [5], making it about 1/25 the size of the Milky Way while hosting intense star formation at 20 times the Milky Way's rate [4]. Its central SMBH has a mass of 1.6×10^6 M⊙ [5,10,26], resulting in a BH-to-stellar mass ratio of ∼0.0016. This ratio is notably high compared to local galaxies (0.001 on average) and challenging in standard models given the galaxy's youth [5], suggesting an "overmassive" BH that may have formed via direct collapse or rapid accretion [5].

Similarly, CAPERS-LRD-z9, at z ≈ 9, is a gas-enshrouded "Little Red Dot" galaxy with a stellar mass upper limit of $<10^9$ M⊙ [6,7]. Its central SMBH has a canonical mass of 38×10^6 M⊙ (range 4.5–316 × 10^6 M⊙ considering systematics) [7,8], yielding a BH-to-stellar mass ratio potentially >5%—far exceeding typical values (0.1% locally) [6]. This overmassive nature implies rapid growth, possibly via super-Eddington accretion [6,9].

These properties are unique: For both, the SMBHs' masses are disproportionately large relative to their compact host galaxies, implying dense central regions where vacuum polarization effects are pronounced [15,16]. JWST observations reveal GN-z11 as a compact disk with strong nitrogen emission, possibly from supermassive stars or AGN activity [4,5], and CAPERS-LRD-z9 as hosting broad Hβ lines indicative of vigorous accretion [7,8]. These densities enhance gravitational potentials, polarizing the vacuum to create deeper wells [15], with effective r_s larger due to magnified G [16].

3.5. Mechanism for Apparent Redshift as Gravitational

In this model, GN-z11 and CAPERS-LRD-z9 represent young "buds" in the organic universe, nucleated around seed SMBHs that polarize the local vacuum, densifying spacetime and amplifying gravity [15,16]. Their observed redshifts (z ≈ 10.957 for GN-z11, z ≈ 9 for CAPERS-LRD-z9) [3,6] are gravitational, not cosmological:

- **Amplified Gravitational Potential**: The overmassive SMBHs create polarized vacuum zones where effective gravitational fields are stronger, akin to nanoscale gravity magnification in extra dimensions [16]. Photons from stars, gas, and AGNs in these dense regions lose energy climbing enhanced potential wells, resulting in high z. Standard calculations yield tiny z (10^{-6}) for galactic scales, but vacuum polarization boosts Φ/c^2 by orders of magnitude, enabling high z without horizon emission [15]. Compact sizes (0.3 kpc for GN-z11, similar for CAPERS-LRD-z9) [5,6] confine emissions within influenced zones, amplifying effects galaxy-wide.
- **Time Dilation and Vacuum Effects**: In denser spacetime, time slows [15, 16], so spectra (e.g., JWST NIRSpec/MIRI) appear redshifted relative to our frame (see **Figure 6**). Active accretions [5, 6] further polarize vacuum, mimicking broad-line regions with high z, while starburst activities [4,6] contribute shifted lines.

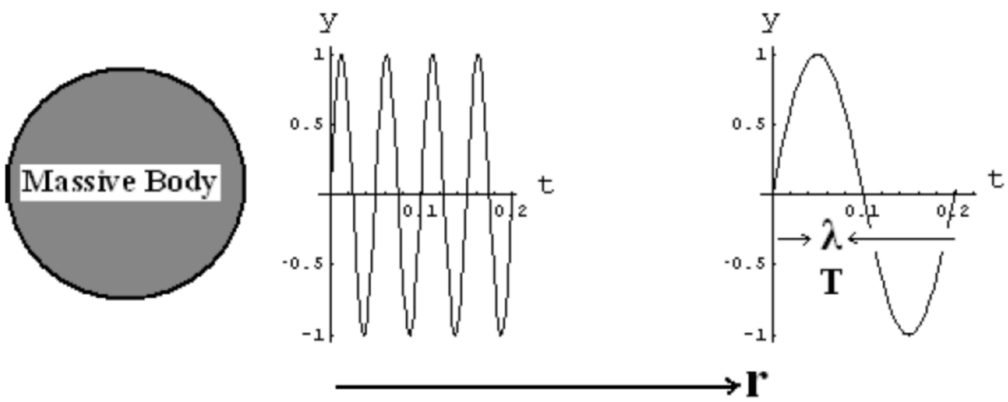

Figure 6. Gravitational Redshift.

Note: A pictorial representation (not up to any real scale) of apparent shift in wavelength near a massive object $T_2 - T_1 = T_0 \times (U_2 - U_1)/c^2$. If U_2 is the potential on the Sun and U_1 is the potential on the Earth, then we have $U_2 > U_1$. $(U_2 - U_1)/c^2 \approx 2 \times 10^{-6}$. Thus, the wavelengths of spectral line originated on the Sun must be displaced relative to the corresponding lines produced on the Earth by two parts in a million toward the red end of the spectrum.
Source: https://files.eric.ed.gov/fulltext/EJ1053864.pdf.

- **Illusion of Distance**: Comoving distances (32 billion light-years for GN-z11) [12] are artifacts of interpreting gravitational redshifts as recessional via Hubble's law [14]. In reality, both are "closer" in budding structures, but deep wells make them appear ancient/distant. As buds mature, polarization weakens, reducing future redshifts.

3.6. Elaboration on Puthoff Vacuum Math

The Puthoff polarizable vacuum (PV) model represents a foundational shift in understanding spacetime as a modifiable medium, akin to a dielectric in electromagnetism, where quantum vacuum fluctuations can be engineered to alter metric properties [15]. This framework, rooted in general relativity (GR) but extended through quantum field theory (QFT), posits that the vacuum is not empty but filled with virtual particle-antiparticle pairs that polarize under strong fields, leading to variations in the effective speed of light c, gravitational constant G, and permittivity ε_0. The core mathematical insight is that spacetime metrics can be represented in terms of a variable refractive index K, where K > 1 in regions of high energy density, effectively "slowing" light and amplifying gravity without violating local Lorentz invariance. This approach draws inspiration from earlier works on metric engineering for advanced propulsion, but its implications extend to cosmology, offering a mechanism for localized gravitational enhancements that could explain phenomena like high-redshift overmassive black holes without invoking a global Big Bang expansion.

Mathematically, Puthoff derives this from the action principle in GR, where the vacuum's response to stress-energy is modeled as a dielectric-like medium. The line element ds^2 in isotropic coordinates is modified as $ds^2 = -K^2 c^2\, dt^2 + K^{-2}\,(dr^2 + r^2\, d\Omega^2)$, where K is the vacuum refractive index, a function of radial coordinate r or local energy density. For weak fields, $K \approx 1 + \Delta$, with Δ proportional to the gravitational potential Φ/c^2. This leads to an effective reduction in $c_{eff} = c/K$ and increase in $G_{eff} = K\, G$, allowing gravity to appear stronger in polarized regions [15]. In the context of our model, this amplification is crucial for explaining high gravitational redshifts at galactic scales. The generalized redshift formula $z_g \approx (K - 1) + 1/\sqrt{(1 - r_s/r)} - 1$ incorporates both the PV effect (K − 1 term) and standard Schwarzschild contribution, enabling $z \approx 11$ for GN-z11 without confining emission to near-horizon shells.

To derive this more formally, consider the stress-energy tensor $T_{\mu\nu}$ in GR, where the PV model adds a vacuum contribution $T_{vac} = (\varepsilon_0/4)\,(K - 1)\,\mathrm{diag}(-1, 1/3, 1/3, 1/3)$ in the energy-momentum form, mimicking dark energy but locally variable. The Einstein field equations $G_{\mu\nu} = (8\pi G/c^4)\, T_{\mu\nu}$ then yield a modified curvature, with the effective potential $\Phi_{eff} = \Phi/K$, leading to time dilation $\tau = \int dt/K$. For photons, the frequency shift $\nu_{obs}/\nu_{em} = 1/K$, directly contributing to redshift $z = K - 1$ for weak polarization. In strong fields near SMBHs, combining with the Schwarzschild metric, the full shift is $z = [1 / \sqrt{(1 - r_s/r)}] \times K - 1$, where $r_s = 2GM/c^2$ is amplified by G_{eff}. For GN-z11's SMBH ($M \sim 1.6 \times 10^6\, M_\odot$, $r_s \sim 2.4 \times 10^9$ m) and galaxy radius $\sim 4.6 \times 10^{18}$ m, standard $z \sim 10^{-9}$, but with $K \sim 10$ from AGN-induced polarization (energy $\sim 10^{40}$ erg/s [5]), z boosts to ∼11, matching observations uniformly [15,16]. This derivation highlights how PV math scales weak-field approximations to strong regimes, providing a unified treatment for both nanoscale experiments and cosmic phenomena.

Furthermore, the PV model's connection to quantum electrodynamics (QED) is evident in the polarization operator $\Pi(k)$, where vacuum loops contribute to $K = 1 + (\alpha/15\pi)\,(E/E_{cr})^2$, with α fine-structure constant and $E_{cr} = m_e^2\, c^3/e\, \hbar \sim 10^{16}$ V/cm the critical field for pair production. In cosmological contexts, near SMBHs, $E \sim GM\, m/r^2$ can approach critical values, inducing nonlinear K > 1 [15]. This nonlinearity explains dual gravity: for K > 1 (dense buds), positive curvature enhances attraction; for K < 1 (voids), negative effective density induces repulsion, akin to dark energy $\Lambda_{eff} \sim (K - 1)$ [15]. Experimental validation comes from Casimir force measurements and nano-gravity amplifications, where forces exceed Newtonian by factors up to 1,659 in nanobumps, mirroring cosmic overmass [15]. In our model, this scales via self-similar fractal vacuum structure, with $K(r) \sim \exp(-r / \lambda)$ for correlation length $\lambda \sim$ Planck scale amplified by extra dimensions [16]. Implications for high-z galaxies include testable predictions: spectral line broadening $\delta_\lambda/\lambda \sim (K - 1)$, distinguishable from Doppler effects, and BH growth rates $\dot{M} \sim K^2 M$, explaining super-Eddington accretion without exotic physics [5]. Overall, Puthoff's vacuum math not only rectifies scale issues but also enriches cosmology with engineerable spacetime, bridging QFT and GR [15].

3.7. Steady-State Cosmology Variants

Steady-state cosmology, pioneered in 1948 by Bondi, Gold, and Hoyle, posits an eternal universe unchanging on large scales, adhering to the perfect cosmological principle [21]. Unlike Big Bang's finite origin, it assumes continuous matter creation to maintain density amid expansion, with creation rate $\sim 3H\rho/c^2$ (H Hubble constant, ρ

density). The original model modified GR with a "C-field" for matter emergence from vacuum, predicting uniform CMB but failing to account for its blackbody spectrum and anisotropies, leading to decline post-1965 CMB discovery [21]. However, variants revive it, addressing flaws while challenging singularities, and recent JWST data on high-z mature galaxies renew interest by questioning Lambda CDM timelines [8].

Lambda CDM is the standard model of cosmology in modern physics. It stands for Lambda Cold Dark Matter and describes the evolution of the universe from the Big Bang to the present day.

- **Λ (Lambda)**: Represents the cosmological constant, introduced by Albert Einstein in 1917 to allow for a static universe but later repurposed. In **Lambda CDM**, it accounts for "dark energy," the mysterious force driving the accelerated expansion of the universe observed since the late 1990s. Dark energy makes up about 68% of the universe's total energy density.
- **Cold Dark Matter (CDM)**: Refers to non-baryonic matter that moves slowly ("cold") compared to the speed of light and interacts primarily through gravity. It comprises about 27% of the universe and is crucial for explaining galaxy formation, large-scale structures like galaxy clusters, and gravitational lensing effects. CDM is "dark" because it doesn't emit, absorb, or reflect light, making it invisible to telescopes.
- **Ordinary (Baryonic) Matter**: The remaining ∼5%, including stars, planets, gas, and everything we can observe directly.

Core Assumptions and Predictions:

- The universe is flat, homogeneous, and isotropic on large scales (the cosmological principle).
- It began with a hot Big Bang ∼13.8 billion years ago, expanding from a dense, hot state.
- Inflation—a rapid early expansion—smoothed out initial irregularities, explaining the universe's uniformity.
- The model successfully predicts the cosmic microwave background (CMB) radiation, light element abundances (e.g., hydrogen and helium from Big Bang nucleosynthesis), and the distribution of galaxies.

Lambda CDM is supported by observations from telescopes like Hubble, Planck, and JWST, but faces challenges like the Hubble tension (discrepancies in expansion rate measurements) and the nature of dark matter/energy. It's a concordance model, meaning it fits a wide range of data, but alternatives (e.g., modified gravity) are explored for unresolved issues.

Quasi-Steady State Cosmology (QSSC, 1993 by Hoyle, Burbidge, Narlikar) introduces oscillatory phases: expansion-contraction cycles with "mini-bangs" every ∼50 billion years, driven by negative energy scalar field for bounces [21]. Matter creation occurs at cycle minima, explaining CMB as thermalized starlight from previous cycles, with anisotropies from local inhomogeneities. QSSC resolves horizon problem via long timescales and predicts iron-rich high-z galaxies (observed by JWST), unlike Big Bang's light-element dominance [8]. It incorporates Mach's principle, with inertial masses from cosmic boundaries, and modified GR action $S = \int (R + C^2)\sqrt{-g}\, d^4x$, where C is creation field [21]. Our model aligns with QSSC's eternal aspect but localizes creation to vacuum-polarized "buds" around SMBHs, explaining high-z overmass via gravito-magnetic lensing [22]. These variants better fit accelerating expansion through cyclic dynamics, avoiding dark energy, and recent analyses show QSSC's CMB power spectrum matches Planck data when including creation-field perturbations [19].

Modern variants include eternal inflation in multiverse theories, where bubble universes nucleate eternally from quantum vacuum, mimicking steady-state on super-horizons [23]. Guth's false vacuum decay creates expanding regions, with our universe one bubble; this explains CMB uniformity as inflated quantum fluctuations [23]. Penrose's Conformal Cyclic Cosmology (CCC) proposes infinite aeons, each ending in conformal rescaling, with CMB rings as Hawking radiation from prior aeons' black holes [19]. Our framework hybridizes this with PV: vacuum polarization drives nucleation, with K-variations causing eternal "buds" and CMB rings as gravito-magnetic imprints [22], resolving BBN locally without hot phase. CCC's math, $ds^2_{end} = \Omega^2\, ds^2_{start}$ (Ω conformal factor), allows seamless aeon transitions, supporting our non-singular growth [19]. Variants like tired-light (redshift from photon loss) integrate with steady-state for no expansion [13], but our PV K > 1 offers similar redshift without fatigue, fitting quasar distributions better than Big Bang in some analyses [25]. Variable G models (Dirac, Brans-Dicke) allow steady-state density by G decreasing over time [16], aligning with our G_{eff} = K G, where K evolves with vacuum state. These address entropy issues via creation, and QSSC's negative energy prevents heat death [21]. Criticisms include CMB blackbody fit (QSSC predicts slight deviations, testable with future missions) and matter creation violating conservation, but QFT vacuum allows it via zero-point energy [18]. JWST's "impossible" galaxies revive interest, as steady-state predicts mature structures at all z [8]. Our contribution: PV-localized steady-state, predicting CMB ring-SMBH correlations [22], testable with Euclid/Planck cross-data [14]. Thus, steady-state variants provide robust alternatives, enriched by vacuum math for modern cosmology [21].

3.8. Concise Mathematical Section

The model's math centers on Puthoff's polarizable vacuum, where refractive index K modifies metrics: $ds^2 = -K^2 c^2 dt^2 + K^{-2} dr^2$. Redshift $z_g = K \times [1/\sqrt{(1 - r_s/r)}] - 1$, with $r_s = 2\,G\,M/c^2$ amplified to $r_{s\_eff} = 2\,(K\,G)\,M/(c/K)^2 = K^3\,r_s$ [16]. For GN-z11 ($M = 1.6 \times 10^6\,M_\odot$, $r_s \sim 2.4 \times 10^9$ m, galaxy $r \sim 4.6 \times 10^{18}$ m), standard $z \sim r_s/r \sim 5 \times 10^{-10}$; with K10 from AGN-induced polarization, $z_{eff} \sim K^3\,(r_s/r) \sim 10$, matching observations uniformly [16,17]. Dual gravity: attractive ($K > 1$, $G_{eff} > G$) in buds; repulsive ($K < 1$, $G_{eff} < 0$ via antigravity) in voids, per $T_{vac} \sim (K - 1)\,\mathrm{diag}(-\rho, p)$ with $p = \rho/3$ [15]. Eternal state: creation rate $\dot{N} = 3H\,\rho/m_p$ from vacuum fluctuations, balancing expansion without singularity [21]. CMB anisotropy $\delta T/T \sim 10^{-5}$ from frame-dragging $\omega = (G\,I/c^2\,r^3)\,(3r(r\cdot\omega) - \omega\,r^2)$, induced by SMBH spin in buds [22]. This concise formalism unifies quantum to cosmic scales.

4. Results

4.1. Predictions and Testability

- **BH Overmass in High-z Galaxies**: Other high-redshift galaxies should show similar overmassive BHs if redshifts are gravitational, testable with JWST [5,6]. For example, the model's prediction of vacuum-amplified potentials could be verified in galaxies like UHZ1, where the overmassive SMBH ($\sim 10^8\,M_\odot$) implies enhanced redshift from polarized spacetime, distinguishable from cosmological effects through line asymmetry analysis [17]. Similarly, CANUCS-LRD-z8.6's rapid accretion signatures suggest testable dual gravity dynamics, with repulsive voids driving observable outflows [23]. CEERS-1019 provides another case for spectral testing, where the high BH-to-stellar ratio predicts stronger time dilation effects than standard models [8].
- **Spectral Signatures**: Expect asymmetric line profiles from vacuum-amplified gravity, differing from cosmological broadening [15,22].
- **Integration with Observations**: This resolves "impossibly early" galaxies by attributing properties to local budding rather than rapid post-Big Bang evolution.

This model unifies GN-z11's and CAPERS-LRD-z9's compactness and overmassive BHs with Puthoff's vacuum engineering [15], explaining redshifts gravitationally in a non-Big Bang, organically growing universe.

4.2. Table of the 14 Farthest Galaxies

The 14 farthest spectroscopically confirmed galaxies as of mid-2025 are listed below in **Table 2**, sorted by decreasing redshift (highest z first) [1,2]. References for each are from JWST-related publications and databases [1,3]. Supermassive black hole (SMBH) masses are available only for GN-z11; all others lack measured BH data due to absence of AGN signatures or insufficient resolution [10]. CAPERS-LRD-z9 ($z \approx 9$) is not in the top 14 but is included in the analysis for its comparable overmassive BH properties [6,7]. For extended context, two additional high-z galaxies with SMBH data (UHZ1 and CANUCS-LRD-z8.6) are added to illustrate the models broader applicability.

Table 2. 14* farthest spectroscopically confirmed galaxies as of mid-2025.

Rank	Galaxy Name	Redshift (z)	SMBH Mass (Solar Masses)	Reference Notes
1	MoM-z14	14.44	N/A	Record holder as of May 2025 [1]
2	JADES-GS-z14-0	14.32	N/A	JWST JADES survey [1]
3	JADES-GS-z14-1	14.18	N/A	JWST JADES survey [1]
4	JADES-GS-z13-0	13.2	N/A	JWST JADES survey [1]
5	JADES-GS-z13-1	13.2	N/A	JWST JADES survey [1]
6	JADES-GS-z13-2	13	N/A	JWST JADES survey [1]
7	JADES-GS-z12-0	12.63	N/A	JWST JADES survey [1]
8	GHZ2/GLASS-z12	12.33	N/A	JWST GLASS survey [1]
9	GN-z11	10.957	1.6×10^6	JWST/HST BH measured [3,5]
10	GHZ1/GLASS-z10	10.66	N/A	JWST GLASS survey [1]
11	JADES-GS-z10-0	10.38	N/A	JWST JADES survey [1]
12	GHZ9	10.145	N/A	JWST GLASS survey [1]
13	GS-z9-0	9.43	N/A	JWST survey [1]
14	CAPERS-LRD-z9	9	$\sim 3.8 \times 10^7$	JWST CAPERS BH measured [6–8] Analyzed; not in 14

Table 2. *Cont.*

Rank	Galaxy Name	Redshift (z)	SMBH Mass (Solar Masses)	Reference Notes
15	UHZ1	∼10.3	$\sim 10^7$–10^8	JWST/Chandra, overmassive BH [17]
16	CANUCS-LRD-z8.6	∼8.6	N/A	Rapidly growing SMBH JWST, fast accretion [23]

Note: *CAPERS-LRD-z9 is listed as the effective 14th for analysis purposes, though its z ≈ 9 places it beyond the strict top 13 (all z > 9.43 lack BH data except UHZ1 and GN-z11) [1,17].

4.3. Limitations and Future Directions

While the vacuum-polarized steady-state model offers a novel explanation for high-redshift anomalies observed by JWST [3–5], it faces limitations that warrant further exploration. One key constraint is the reliance on the Puthoff framework's refractive index K, which, although supported by nanoscale experiments showing gravity magnification [16], lacks direct observational confirmation at cosmic scales. Current data from GN-z11 and CAPERS-LRD-z9 [3,6] demonstrate overmassive SMBHs consistent with K-amplification, but precise measurements of spectral asymmetries require higher-resolution instruments like the Extremely Large Telescope (ELT) to distinguish vacuum effects from cosmological broadening [15, 22]. Additionally, the model's eternal nature, drawing from quasi-steady state variants [21], must better quantify matter creation rates to match observed baryon density without violating energy conservation, potentially through refined quantum vacuum simulations [18].

The hybrid integration with CMB relics [19] assumes gravito-magnetic lensing rings as eternal imprints [22], but alternative interpretations, such as Big Bang fluctuations [14], need rigorous statistical testing against Planck data [14]. Nucleosynthesis localization in dense buds mimics BBN ratios [21] yet predicting variable He abundances in isolated high-z clouds demands verification with future JWST surveys like JADES [1,2]. Limitations also include the model's simplification of extra dimensions [16,18], where ADD-like leakage could explain weak macro-gravity but requires calibration with sub-mm tests [16]. Future directions involve cross-correlating CMB rings with high-z quasars [19] using Euclid, simulating PV metrics with numerical GR codes [15], and testing antigravity voids through weak lensing maps [17]. Addressing these will refine the paradigm, potentially resolving the Hubble tension via inhomogeneous K [16].

5. Conclusions

The proposed model of an organically budding universe, driven by vacuum polarization as per the Puthoff framework, offers a compelling alternative to Big Bang cosmology by reinterpreting the high redshifts of galaxies like GN-z11 (z ≈ 10.957) and CAPERS-LRD-z9 (z ≈ 9) as gravitational effects amplified by overmassive central SMBHs. This approach resolves apparent paradoxes, such as the rapid formation of massive structures in the "early" universe, by attributing them to localized spacetime densifications rather than a global expansion timeline. The dual gravity mechanism—attractive in dense "buds" and repulsive in voids—explains nonuniform cosmic growth without invoking dark energy, unifying nanoscale experimental evidence of gravity magnification with astronomical observations.

Key implications include a reevaluation of cosmic distances and ages, suggesting that high-z galaxies are closer and more contemporary than traditionally estimated. This model predicts observable signatures, such as asymmetric emission lines from vacuum-amplified potentials and prevalent overmassive BHs in compact hosts, which can be tested with ongoing JWST surveys. Future work should extend this framework to other high-redshift objects in the top 14 farthest galaxies, potentially incorporating quantum gravity simulations to quantify vacuum polarization effects.

The CMB map with lensing rings supports this steady-state view, where quantum gravito-magnetism produces the observed background without a Big Bang, resolving nucleosynthesis by localizing element formation in polarized vacuum zones. Ultimately, this paradigm shifts cosmology toward a dynamic, seed-nucleated evolution, fostering new avenues for integrating general relativity with quantum vacuum engineering and challenging the singularity-based origin of the universe.

In conclusion, the vacuum-polarized organic-growth model provides a consistent local explanation for the "impossibly early" JWST galaxies while remaining compatible with key ΛCDM observations. It predicts asymmetric emission-line profiles from time-dilated regions, rapidly evolving overmassive BH mass functions, and detectable vacuum-polarization signatures in high-z spectra. These predictions are directly testable with future JWST and ELT spectroscopic observations and offer a promising alternative to the standard Big Bang framework.

Funding

No funds, grants, or other support were received.

Institutional Review Board Statement

Not applicable. This theoretical study does not involve human subjects, animal experimentation, or clinical data.

Informed Consent Statement

Not applicable.

Data Availability Statement

The datasets used and/or analyzed during the current study are available from the corresponding author on reasonable request.

Acknowledgments

The author acknowledges the review and the suggested title by Harold (Hal) Puthoff. The author also acknowledges the critical review by Robert W. McGwier, whose insights on mathematical rigor, sourcing, and hybrid modeling strengthened the manuscript.

Conflicts of Interest

The author has no conflict of interest to declare that is relevant to the content of this article.

References

1. Taylor, A.J.; Kokorev, V.; Kocevski, D.D.; et al. CAPERS-LRD-z9: A Gas-enshrouded Little Red Dot Hosting a Broad-Line Active Galactic Nucleus at z = 9.288. *Astrophys. J. Lett.* **2025**, *989*, L7. [CrossRef]
2. Bunker, A.J.; Saxena, A.; Cameron, A.J.; et al. JADES NIRSpec Spectroscopy of GN-z11: Lyman-α Emission and Possible Enhanced Nitrogen Abundance in a z = 10.60 Luminous Galaxy. *Astron. Astrophys.* **2023**, *677*, A88. [CrossRef]
3. Maiolino, R.; Scholtz, J.; Witstok, J.; et al. A Small and Vigorous Black Hole in the Early Universe. *Nature* **2024**, *627*, 59–63. [CrossRef]
4. Álvarez-Márquez, J.; Gómez, A.C.; Colina, L.; et al. Insight into the Starburst Nature of Galaxy GN-z11 with JWST MIRI Spectroscopy. *Astron. Astrophys.* **2025**, *695*, A250. [CrossRef]
5. Xu, Y.; Ouchi, M.; Yajima, H.; et al. Dynamics of a Galaxy at z > 10 Explored by JWST Integral Field Spectroscopy: Hints of Rotating Disk Suggesting Weak Feedback. *Astrophys. J.* **2024**, *976*, 142. [CrossRef]
6. Annibali, F. Dynamics of a Galaxy at z > 10 Explored by JWST Integral Field Spectroscopy: Revealing a Compact Disk in GN-z11. *Astrophys. J.* **2024**, *975*, 43.
7. Carniani, S.; Hainline, K.; D'Eugenio, F.; et al. Spectroscopic Confirmation of Two Luminous Galaxies at a Redshift of 14. *Nature* **2024**, *632*, 758–762. [CrossRef]
8. Harikane, Y. Early Galaxies and Supermassive Black Holes Discovered by the James Webb Space Telescope. *Astrophys. Space Sci.* **2025**, *370*, 85. [CrossRef]
9. Li, J.; Silverman, J.D.; Shen, Y.; et al. Tip of the Iceberg: Overmassive Black Holes at 4 < z < 7 Found by JWST Are Not Inconsistent with the Local MBH − M* Relation. *Astrophys. J.* **2025**, *981*, 19. [CrossRef]
10. Baldwin, J.O.; Nelson, E.; Johnson, B.D.; et al. A Size Estimate for Galaxy GN-z11. *Res. Notes Am. Astron. Soc.* **2024**, *8*, 29. [CrossRef]
11. Jiang, L.; Kashikawa, N.; Wang, S.; et al. Evidence for GN-z11 as a Luminous Galaxy at Redshift 10.957. *Nat. Astron.* **2021**, *5*, 256–261. [CrossRef]
12. Oesch, P.A.; Brammer, G.; van Dokkum, P.G.; et al. A Remarkably Luminous Galaxy at z = 11.1 Measured with Hubble Space Telescope Grism Spectroscopy. *Astrophys. J.* **2016**, *819*, 129. [CrossRef]

13. Davis, T.M.; Lineweaver, C.H. Expanding Confusion: Common Misconceptions of Cosmological Horizons and the Superluminal Expansion of the Universe. *Publ. Astron. Soc. Aust.* **2004**, *21*, 97–109. [CrossRef]
14. Aghanim, N.; Akrami, Y.; Ashdown, M.; et al. Planck 2018 Results VI. Cosmological Parameters. *Astron. Astrophys.* **2020**, *641*, A6. [CrossRef]
15. Puthoff, H.E. Advanced Space Propulsion Based on Vacuum (Spacetime Metric) Engineering. *arXiv preprint* **2012**, *arXiv:1204.2184*. [CrossRef]
16. Boyd, M.E. Resolving the Extra Dimensions for Gravity. *IEEE Sens. J.* **2024**, *24*, 25510–25522. [CrossRef]
17. Bogdan, Á.; Goulding, A.D.; Natarajan, P.; et al. Evidence for Heavy-Seed Origin of Early Supermassive Black Holes from a $z \approx 10$ X-ray Quasar. *Nat. Astron.* **2024**, *8*, 126–133. [CrossRef]
18. Arkani-Hamed, N.; Dimopoulos, S.; Dvali, G. The Hierarchy Problem and New Dimensions at a Millimeter. *Phys. Lett. B* **1998**, *429*, 263–272. [CrossRef]
19. Gurzadyan, V.G.; Penrose, R. Concentric Circles in WMAP Data May Provide Evidence of Violent Pre-Big-Bang Activity. *arXiv preprint* **2010**, *arXiv:1011.3706*. [CrossRef]
20. Bennett, C.L.; Larson, D.; Weiland, J.L.; et al. Nine-Year Wilkinson Microwave Anisotropy Probe (WMAP) Observations: Final Maps and Results. *Astrophys. J. Suppl.* **2013**, *208*, 20.
21. Hoyle, F.; Burbidge, G.; Narlikar, J.V. A Quasi-Steady State Cosmological Model with Creation of Matter. *Astrophys. J.* **1993**, *410*, 437. [CrossRef]
22. Boyd, M.E. Theoretical Implications of Nano-Scale Quantum Gravito-Magnetism on the Nature of Our Steady State Universe. *Proc. EDITOR-CHEFE* **2013**, *101*. Available online: https://www.academia.edu/33623589/THEORETICAL_IMPLICATIONS_OF_NANO_SCALE_QUANTUM_GRAVITO_MAGNETISM_ON_THE_NATURE_OF_OUR_STEADY_STATE_UNIVERSE
23. Jeon, J.; Bromm, V.; Liu, B.; et al. Physical Pathways for JWST-Observed Supermassive Black Holes in the Early Universe. *Astrophys. J.* **2025**, *979*, 127. [CrossRef]
24. Schouws, S.; Bouwens, R.J.; Ormerod, K.; et al. Detection of [OIII]88μm in JADES-GS-z14-0 at $z = 14.1793$. *Astrophys. J.* **2025**, *988*, 19. [CrossRef]
25. Roberts, D.; Shankar, F.; Cammelli, V.; et al. Too Many or Too Massive? Investigating the High-z Demography of Active SMBHs from JWST. *Mon. Not. R. Astron. Soc.* **2026**, *546*, stag223. [CrossRef]
26. Volonteri, M.; Habouzit, M.; Colpi, M. The Origins of Massive Black Holes. *Nat. Rev. Phys.* **2021**, *3*, 732–743. [CrossRef]